BBA Biomembranes

The impact of the C-terminal domain on the gating properties of MscCG from *Corynebacterium glutamicum*

Yoshitaka Nakayama [a], Michael Becker [b], Haleh Ebrahimian [a, c], Tomoyuki Konishi [d], Hisashi Kawasaki [d], Reinhard Krämer [b], Boris Martinac [a]

a. Victor Chang Cardiac Research Institute, Darlinghurst, Sydney, NSW 2010, Australia

b. Institute of Biochemistry, University of Cologne, Zulpicher Str. 47, 50674 Koln, Germany

c. Wollongong University, Sydney, NSW 2010, Australia

d. Department of Green and Sustainable Chemistry, Tokyo Denki University, 5 Asahi-cho, Senju, Adachi-ku, Tokyo 120-8551, Japan

Corresponding author:

Boris Martinac

b.martinac@victorchang.edu.au

Keywords:

NCgl1221, Mechanosensitive channel, Glutamate efflux, Gating hysteresis, *E. coli*, spheroplasts, Liposomes, Patch clamp.

Abstract

The mechanosensitive (MS) channel MscCG from the soil bacterium *Corynebacterium glutamicum* functions as a major glutamate exporter. MscCG belongs to a subfamily of the bacterial MscS-like channels, which play an important role in osmoregulation. To understand the structural and functional features of MscCG, we investigated the role of the carboxyl-terminal domain, whose relevance for the channel gating has been unknown. The chimeric channel MscS-(C-MscCG), which is a fusion protein between the carboxyl terminal domain of MscCG and the MscS channel, was examined by the patch clamp technique. We found that the chimeric channel exhibited MS channel activity in *E. coli* spheroplasts characterized by a lower activation threshold and slow closing compared to MscS. The chimeric channel MscS-(C-MscCG) was successfully reconstituted into azolectin liposomes and exhibited gating hysteresis in a voltage-dependent manner, especially at high pipette voltages. Moreover, the channel remained open after releasing pipette pressure at membrane potentials physiologically relevant for *Corynebacterium glutamicum*. This contribution to the gating hysteresis of the C-terminal domain of MscCG confers to the channel gating properties highly suitable for release of intracellular solutes.

Introduction

Osmoregulation is one of the indispensable stress responses in living cells. In bacterial cells water influx by hypo-osmotic shock increases suddenly the cell volume and causes cell lysis. Bacterial cells respond to osmotic stress mainly by opening mechanosensitive (MS) channels of small conductance, MscS, and of large conductance, MscL, which function as osmotic safety valves [1,2,3]. These channels are activated by increased membrane tension upon hypo-osmotic shock, and release intracellular compatible solutes, such as betaine, and ions to reduce the osmotic gradient [4]. On the other hand, the export of the intracellular molecules is controlled to maintain ion homeostasis by regulation of channel gating. Therefore, MscS exhibits desensitization and inactivation mechanisms [5,6], and these functions contribute to the survival of bacterial cells under hypo-osmotic stress [7]. Members of the MscS-family of proteins are found in cell-walled organisms from bacteria to plants and function largely in the hypo-osmotic cellular response [8,9,10,11,12].

The aerobic Gram-positive soil bacterium *Corynebacterium glutamicum* secretes a massive amount of glutamate when the cellular envelope, i.e. the cell-membrane or the cell-wall, is structurally compromised [13,14,15,16]. Glutamate fermentation from *C. glutamicum* is utilized worldwide for industrial glutamate production and glutamate is produced as a seasoning evoking umami taste, one of the five basic tastes. Despite the importance for industrial glutamate production, the mechanism of glutamate export has not been understood for a long time. However, the situation has changed significantly since MscCG (NCgl1221) was identified by screening of glutamate-overproducing strain of *C. glutamicum* [17] and functionally characterized as a mechanosensitive channel [18]. Under biotin-limitation culture, addition of penicillin or Tween-40, *C. glutamicum* exports glutamate passively

through MscCG [17,19,20]. In addition, some mutations in MscCG cause constitutive glutamate secretion [17,20].

The MscCG-type channel is a member of the MscS-like channel family, and the most characteristic feature of this channel is the presence of an extended C-terminal domain, which includes a fourth TM4 transmembrane helix compared to only three transmembrane helices in the canonical MscS [18,20]. This extended domain is exclusively found in MscS-like proteins from *Corynebacterium* species and indicates its significance for glutamate production [21]. Patch clamp experiments showed that MscCG expressed heterogeneously in *E. coli* spheroplasts and *B. subtilis* provacuoles exhibited gating characteristics different from MscS [18,19,22]. MscCG showed stronger gating hysteresis than MscS and neither desensitization nor inactivation of the channel were observed when the channel was expressed in *E. coli* spheroplasts [18,23]. The functional and structural differences between MscCG and MscS have at present not been well understood.

The role of the C-terminal domain for the function of MscCG has been puzzling. Becker *et al.* reported a significant effect on the glutamate export in *C. glutamicum* expressing the chimeric channel MscS-(C-MscCG), which is a fusion protein consisting of the C-terminal domain of MscCG (287-533 a.a.) and *E. coli* MscS (1-286 a.a.). Furthermore, Yamashita *et al* have reported that spontaneous glutamate export is induced when the periplasmic loop (419-533 a.a.) of the C-terminal domain of MscCG is truncated [24]. In addition, they demonstrated that MscCG has an extra loop (221-232 a.a.) predicted by homology modelling in the N-terminal cytoplasmic domain, which MscS does not have, and this extra loop is necessary for the glutamate export and may interact with the C-terminal domain [24, 25] (Fig. 1A). Recently, a full-size analysis of the C-terminal domain of MscCG has been performed with deletion of subdomains, replacement of segments by other amino

acid sequences, and sequence randomization. All subdomains of the C-terminal domain, the periplasmic loop, the fourth transmembrane segment, and the cytoplasmic loop, were proved to be significant for glutamate export [26]. Together these findings suggest that the C-terminal domain plays roles in the gating of MscCG by modulating glutamate export effectively. Finally, it is also important to mention that the N-terminal domain of MscCG (1-286 a.a.), which includes the channel pore, is essential for the glutamate export based on experiments performed on truncated, gain-of-function (GOF) and loss-of-function (LOF) MscCG mutants [18,20].

In this study, we examined the role of the C-terminal domain in the MscCG gating by patch clamp electrophysiology in *E. coli* spheroplasts and azolectin liposomes. To this end the activation thresholds, ion conductance, and gating kinetics of the C-terminally truncated MscCG and chimeric channel MscS-(C-MscCG) were investigated in *E. coli* spheroplasts. In addition, the chimeric MscS-(C-MscCG) channel protein was purified and reconstituted into liposomes and its gating hysteresis was examined at pipette voltages corresponding to physiological membrane potentials in *C. glutamicum*. Our results indicate that the C-terminal domain of MscCG confers to the channel unique gating characteristics important and necessary for glutamate export.

Results

The influence of the C-terminal domain on the gating properties of MscCG and MscS in E. coli spheroplasts

MscCG consists of four transmembrane (TM) domains and a large extension in the C-terminal region, which is missing in MscS that has only three transmembrane helices (Figure 1A). The first transmembrane helix of MscCG is characterized by repeats of arginine residues, whereas the other three helices consist mostly of hydrophobic residues. Between TM3 and TM4, MscCG has a large intracellular region including the extra loop (221-232 a.a.) that seems to be necessary for glutamate transport [24], in addition to several negatively charged residues in the C-terminal domain (Figure 1B).

To investigate whether the C-terminal domain of MscCG plays a role in the activation threshold of the channel, we examined the truncated mutant MscCGΔ247, which is lacking the C-terminal domain as well as the chimeric channel MscS-(C-MscCG) channel in which the MscCG C-terminal domain was fused to the C-terminal end of *E. coli* MscS. We then compared the gating thresholds and ion conductance of these channels with the activation thresholds of the wild-type MscCG and MscS channels. All channels were expressed in MJF431 strain having the genes of MscS, MscK, and MscM deleted (*ΔMscS, ΔMscK, ΔMscM*) and their thresholds for opening and closing were determined in the range of pipette potentials from -60 mV to +80 mV. Due to the slow gating kinetics of MscCG, the threshold of MscCG varied depending on the pressure ramp rate [23]. Therefore, we applied sufficiently slow pressure ramp rate (8 s to the maximum pressure) to the patch membrane using High Speed Pressure Clamp (HSPC) apparatus. The ratio of the first opening pressure against the endogenous activation threshold of the MscL channel present in MJF431 spheroplasts was used to evaluate the threshold for all channels investigated in this study. As shown previously, MscCG exhibited lower activation threshold than MscS [20]. The

threshold ratio of 0.41 ± 0.02 for opening and 0.28 ± 0.02 for closing (N = 10), respectively, was determined at pipette voltage of +40 mV (Figure 2A). Importantly, the thresholds did not change with the pipette voltage in the whole range of voltages used in this study (Figure 2B) indicating their voltage independence. Compared to MscCG, MscCGΔ247 showed higher threshold ratio for both opening (0.70 ± 0.01) and closing (0.53 ± 0.04) (N = 7) similar to MscS (Fig. 2B). The channel conductance calculated from the current-voltage relationship did not differ between these two channels (Figure 2C). These results suggest that the C-terminal domain of MscCG contributes to the activation thresholds of MscCG in a voltage independent manner. The chimeric channel MscS-(C-MscCG) exhibited threshold for opening (0.47 ± 0.02, N = 7) similar to MscCG rather than MscS (0.62 ± 0.06, N = 7) at +40 mV (Figure 2A). Interestingly, the threshold for closing of MscS and MscS-(C-MscCG) decreased as the pipette voltage was increased. Furthermore, the chimeric channel MscS-(C-MscCG) did not close at +80 mV even if the pressure applied to the patch pipette was completely removed (Figure 2B), whereas MscS did. The current-voltage relationship for MscS-(C-MscCG) did not differ from that of MscS (Figure 2C). These results suggest that the C-terminal domain of MscCG affects the opening and closing thresholds of the chimeric channel in a voltage-independent and voltage-dependent manner, respectively.

In order to examine whether the fourth transmembrane helix TM4 is important for setting the activation threshold of MscCG, we replaced TM4 of MscCG with an artificial transmembrane helix of human glycophorin [26, 27]. Threshold ratio of the channel containing the glycophorin transmembrane helix (MscCG-hgTM4) was larger (0.70 ± 0.02, N = 5) than the ratio for MscCG and comparable to that of MscCGΔ247 (Figure 3). This result suggests that the fourth transmembrane helix is involved in sensing membrane tension.

The C-terminal region of MscCG enhances gating hysteresis of MscS

Gating hysteresis is one of the unique characteristics of MscCG. Thus we investigated whether the chimeric channel MscS-(C-MscCG) exhibits gating hysteresis similar to MscCG. To evaluate the gating hysteresis of MscS and MscS-(C-MscCG), we applied step pressure protocol to the spheroplast patch membrane of MJF612 (*ΔMscL, ΔMscS, ΔMscK, ΔMscM*) strain expressing MscS or MscS-(C-MscCG) and plotted peak currents against the applied pressure (Figure 4A). Similarly to MscS, MscS-(C-MscCG) exhibited desensitization, manifested in a gradual decrease of the peak current under the constant pressure. The plots of the peak currents were fitted to Boltzmann distribution function. Half activation pressure, P_{mid}, of MscS and MscS-(C-MscCG) was 92.4 mmHg and 59.8 mmHg, respectively (Figure 4B). Thereafter, we applied different pressure ramp rates to the same patch membrane to examine the extent of the gating hysteresis. The pressure rates corresponded to 1, 3, 5, 7, and 9 s required to reach maximum pressure corresponding to the maximal number of activatable channels at the given pressure ramp rate (Figure 4C). To quantify gating hysteresis, we normalized P_{mid} of opening and closing under pressure ramp to P_{mid} obtained under step pressure. Under fast pressure ramp corresponding to 1 s to maximum pressure (80 mmHg/s), P_{mid} for opening and closing of MscS-(C-MscCG) was 64.9 mmHg and 44.1 mmHg respectively, whereas that of MscS was 91.2 mmHg and 81.6 mmHg. This difference in P_{mid} between opening and closing disappeared as the pressure ramp rate was increased (Figure 4D), indicating that MscS-(C-MscCG) exhibited stronger gating hysteresis than MscS. In addition, we analysed the pressure sensitivity for pressure, $1/\alpha$, obtained from the slope at half activation of Boltzmann curve for MscS and MscS-(C-MscCG). $1/\alpha$ for the channel closing of MscS-(C-MscCG) was always larger than that of MscS while $1/\alpha$ for the channel opening was similar for both channels (Figure 4E). These results indicate that the C-terminal domain affects the gating of MscCG by slowing down the closing of the channel.

The glutamate export efficiency of MscCG in E. coli

The lipid membrane of *C. glutamicum* consists of one third of each negatively charged lipids, Phosphatidylglycerol (PG), Phosphatidylinositol (PI), and Cardiolipin (CL) [28], while *E. coli* has a neutral lipid, Phosphatidylethanolamine (PE) as the major component. The differences in lipid components change the mechanical properties of the cell membrane and therefore, not surprisingly the gating of MscS and MscL are affected by the lipid components [29,30]. In order to examine whether MscCG export glutamate in *E. coli* membrane, we measured the glutamate export efficiency of MscCG expressed in *E. coli* cells. The growth of *E. coli* was not affected by the expression of MscCG, however, the glutamate export increased remarkably after 9 h incubation (Figure 5) compared to the strain harbouring the empty vector. This result suggests that MscCG functions as a glutamate exporter also in *E. coli* membrane.

Gating of the chimeric channel MscS-(C-MscCG) at high potential in azolectin liposome

C. glutamicum has very negative resting membrane potential of -170 mV [31] due to an active respiratory chain, and an electrically tight membrane [16]. In order to examine the channel gating at higher pipette voltages than +100 mV of pipette potential, which corresponds to a membrane potential of -100 mV, we attempted to reconstitute all channels examined in this study into azolectin liposomes. Despite a number of trials, we were unable to reconstitute MscCG and MscCGΔ247, however, we were successful in purifying and reconstituting the chimeric MscS-(C-MscCG) channel protein. The MscS-(C-MscCG) protein was detected as a major band of 60kDa as determined by SDS-PAGE (Figure 6A). Pressure ramp was applied to the patch membrane at different pipette voltages ranging from -80 mV to +120 mV. The thresholds for opening and closing of the MscS-(C-MscCG) were determined in the same patch (Figure 6B). The closing threshold of MscS-(C-MscCG) was significantly

reduced at +80 mV. Moreover, at voltages > +100 mV the channel remained open even when the pressure was released. We compared the ratio of pressures corresponding to the first opening and the first closing for MscS and MscS-(C-MscCG), respectively. Similar to the result obtained in *E. coli* spheroplasts, the closing threshold for MscS-(C-MscCG) was significantly reduced compared to that of MscS at +80 mV and +100 mV (Figure 6C). These results indicate that the C-terminal domain of MscCG affects the closing of MscS in a voltage-dependent manner in azolectin liposomes as well. We applied further high pipette potentials up to +160 mV to examine the channel gating at membrane potentials in the vicinity of the resting membrane potential in *C. glutamicum*. At +160 mV, the current trace of MscS-(C-MscCG) changed markedly from its usual bell-shaped profile. Upon reaching the peak, the current decreased gradually without reaching zero current level after releasing the pressure (Figure 6D). The long-lasting current never occurred unless we applied pressure to activate the channel, which indicates that like MscS the MscCG channel is activated by membrane tension but modulated and not activated by voltage [32]. The tendency of gating at high voltages was also seen in MscS and lasted for more than 2 min (Figure 7A). In order to observe carefully the channel currents after ramp pressure, we measured single channel behavior at high voltages. Once MscS opened fully several sub-conducting levels of MscS were observed at +120 and +160 mV and this sub-conducting current continued for an extended period after releasing the pressure, whereas the sub-conducting levels were not observed at +40 and +80 mV (Figure 7B). These results suggest that MscS and MscS-(C-MscCG) once open at a pipette voltage higher than +120 mV they conduct ions also through the sub-conducting states without pressure being applied.

Discussion

In this study, we have investigated the role of the C-terminal domain of MscCG in the channel gating using the patch clamp recording from *E. coli* spheroplasts and azolectin proteoliposomes. The truncation mutant MscCGΔ247 and chimeric channel MscS-(C-MscCG) exhibited activation and deactivation thresholds different from their wild-type counterparts. The most important result from this study indicates that the closing kinetics of the chimeric channel MscS-(C-MscCG) was significantly slower than that of MscS. In addition, the gating hysteresis of MscS was enhanced in a voltage-dependent manner by the presence of the C-terminal domain of MscCG. Furthermore, MscS and MscS-(C-MscCG) remained open after releasing pressure at high pipette potentials > +120 mV. Lower threshold and the gating hysteresis indicative of slower closing of the channels may contribute to the glutamate export in *C. glutamicum* due to increase in the channel open probability. Consequently, we believe that these gating modifications caused by the presence of the C-terminal domain of MscCG can account for the effective glutamate export in *C. glutamicum.*

An increase in the activation threshold of MscCG was observed when the fourth transmembrane helix TM4 of MscCG was replaced with a transmembrane helix of human glycophorin that is unrelated to MscCG and served in this study as a control for the role of TM4 in MscCG mechanosensitivity [20, 25, 31]. The channel containing the glycophorin transmembrane helix (MscCG-hgTM4) required higher pressure for activation compared to wild type MscCG as evidenced by an increase in the pressure ratio for both the opening and the closing threshold of this channel (Figure 3). One possible explanation for this observation is that the glycophorin TM4 helix participates in the channel mechanosensitivity by absorbing some of the membrane tension and thus increasing the total tension required to open this

channel. In support of this view the mutant with the glycophorin TM4 transmembrane helix did not show spontaneous glutamate excretion when overexpressed in contrast to the mutant Δ141 having the TM4 helix deleted [31], which in patch clamp experiments required lower tension for the channel activation [20]. Thus, our data suggest that the C-terminal domain of MscCG contributes to mechanosensitivity of both channels MscCG and MscS in *E. coli* spheroplasts by lowering their threshold of opening as well as closing. Further investigations are, however, required to understand, how MscCG may behave when surrounded by negatively charged lipids during the glutamate export in *C. glutamicum* cells given that, different from *E. coli*, the cell membrane of *C. glutamicum* contains negatively charged lipids, including PG, PI, and CL, as major lipid components. In this context it is worth mentioning that mechanosensitivity of MscS is significantly affected by the presence of CL [30].

Compared to MscS, MscCG has relatively slow gating kinetics and exhibits gating hysteresis under pressure ramp. In MscS-like proteins from eukaryotic cells, such as MSC1 of *Chlamydomonas reinhardtii* and MSL10 of *Arabidopsis thaliana*, the gating hysteresis has been reported as one of unique characteristics of MscS-like proteins [8, 33]. In the MscS case we observed that addition of the C-terminal domain of MscCG slowed the kinetics of MscS closing and did not affect the kinetics of the channel opening. The slow closing kinetics of MscS-(C-MscCG) resulted in the channel staying open longer than wild type MscS. This slow closing corresponds to an increase of the opening time of the channel, which may result in an increased release of intracellular solutes. Consequently, the gating hysteresis observed in MscCG seems to contribute to an efficient export of glutamate in *Corynebacterium glutamicum*.

MscS exhibits strong desensitization and inactivation upon application of membrane tension, which seems well suited for fine-tuning of ion transport upon a hypoosmotic shock rather than for a continuous release of intracellular ions and other solutes. However, we have found that MscS and the chimeric channel MscS-(C-MscCG) in liposomes remained open after releasing pressure at high pipette voltages, suggesting that these channels exhibit increased tendency for solute permeation at voltages in the vicinity of the resting membrane potential of *Corynebacterium glutamicum* of about -170 mV [31]. The kinetics of the channel currents after application of a pressure ramp at high pipette voltages larger than -120 mV was very different from the currents recorded at lower voltages smaller than -80 mV. As previously shown [34] the ionic currents at high pipette voltages largely correspond to subconducting states of MscS reflecting the currents flowing through several of the seven equatorial portals in the channel cytoplasmic vestibule. This is due to negatively charged residues inside the cytoplasmic vestibule proximal to the portals shown to interact with and slow down hydrated cations, which ultimately results in anions becoming predominant carriers of the current through the portals and the pore of the channel [34]. The C-terminal domain of MscCG has many negatively charged residues in the vestibulum, which could play a similar role by attracting hydrated cations around the portals and manifesting in subconducting states of the chimeric channel MscS-(C-MscCG) passing preferentially anions including glutamate. We speculate that this gating characteristic at high negative membrane potentials may be closely involved in the glutamate export in *C. glutamicum*, however, this hypothesis requires further testing.

In summary, the C-terminal domain of MscCG was shown to modulate the gating of MscCG and the MscS-MscCG chimera by decreasing the activation threshold and slowing the closing of the channel, which results in gating hysteresis observed in both of these

channels. This evolutionary modification of the MscCG gating by the addition of an additional negatively charged loop and a transmembrane helix to its C-terminal domain seems to underlie the efficiency of the glutamate release in *C. glutamicum.*

Material and methods

Strains, media and growth

MscCG constructs from *C. glutamicum* ATCC13032 [20] were used for all experiments. *E. coli strain* MJF431 (*Frag1, ΔMscK, ΔMscS, ΔMscM*) [20] and MJF612 (*ΔMscL, ΔMscS, ΔMscK, ΔybdG*) [35] were used for electrophysiology and *E. coli* strain M15 containing pREP4 (Qiagen) and pRARE (Merck) was used for protein purification. All cells were cultured in Luria-Bertani (LB) medium at 37°C, 180 rpm with the incubator INNOVA 44 (Eppendorf).

E. coli spheroplast preparation

E. coli strains MJF431 and MJF612 harbouring the expression plasmid pQE60 lacI with *mscCG* from *C. glutamicum* ATCC13032 were used for preparation of giant spheroplasts as in previous studies [35,36]. Briefly, *E. coli* cells were grown for 1.5 h in the presence of cephalexin, and MscS and MscCG expression was subsequently induced for 5min and 30 min by the addition of 1 mM isopropyl-β-D-thiogalactoside (IPTG), respectively. The cells were harvested and digested with lysozyme. Spheroplasts were collected by centrifugation and stored at -80°C.

Protein purification

MscS and MscS-(C-MscCG) proteins were purified as reported previously [27]. M15 *E. coli* cells containing pREP4 and pRARE were transformed with the expression plasmids, pQE-60, which has lacI coding region for MscS. His-tag was included in the C-terminus of MscS and MscS-(C-MscCG). Cells were cultured in LB medium with the antibiotics, ampicillin 100 μg/ml, kanamycin 12.5 μg/ml, and chloramphenicol 12.5 μg/ml at 37°C until OD_{600} = 1.0, and then induced by the addition of 0.8 mM IPTG in the presence of 0.4% glycerol for

4 h at 25°C. Cells were harvested and resuspended in PBS buffer pH 7.5, and then 200 μg/ml phenylmethanesulfonylfluoride (PMSF) and ~1 mg DNaseI (Sigma-Aldrich) were added and cells were disrupted with a French press (16,000 psi; Thermo Scientific). Lysates were centrifuged to remove cell debris and membranes were collected and solubilized overnight with mixing at 4°C in PBS buffer containing 1 mM n-dodecyl-β-D-maltoside (DDM). The solubilized proteins were purified with immobilized metal affinity chromatography using TALON Co^{2+} sepharose (Clontech, Mountain View, CA). The column was washed with buffer 1 (PBS pH 7.5, 10% glycerol, and 1 mM DDM), followed by buffer 2 (PBS pH 6.0, 10% glycerol, 5 mM imidazole, and 1 mM DDM) twice. The protein was collected using elution buffer containing PBS pH 7.5, 10% glycerol, 300 mM imidazole, and 1 mM DDM. Imidazole was removed by washing the sample twice through an Amicon Ultracentrifugation Device (30 kDa; Millipore, Billerica, MA) with buffer 1 (PBS pH 7.5, 1 mM DDM, and 10% glycerol). The purified protein was stored at 4°C.

Liposome preparation

The Dehydration/Rehydration (D/R) method was carried out as reported in previous studies [37,38]. Briefly, the lipids were dissolved in chloroform and dried with a N_2 gas stream until a thin film of lipid was formed on the wall of a glass tube. Soybean Azolectin (Sigma, P5638 L-α-Phosphatidylcholine from soybean, Type II-S, 14-23% choline basis) was used for the liposome preparation. 2 mg of lipid was dissolved in chloroform and then dried by a stream of N_2 gas. The lipid film was rehydrated by adding 0.2 ml of the D/R solution containing 200 mM KCl and 5 mM HEPES, pH 7.0 (adjusted with KOH). The resulting suspension was vortexed and sonicated for 10 min, which was followed by addition of the appropriate volumes of MscS and MscS-(C-MscCG) to achieve a protein/lipid ratio of 1:500. The volume

was increased to 3 mL using the D/R solution and the tube was placed on an orbital shaker for 1 h at room temperature. Bio-Beads (SM-2; BioRad) were then added and the liposome suspension was further rotated for another 3 h to remove detergent. The suspension was then centrifuged at 250,000 × g for 30 min at 4°C. The pellet was collected, spotted onto a slide glass, and dehydrated under vacuum overnight at 25°C. The dried lipid spot was rehydrated with a 60 μl drop of D/R solution and kept at 4°C for 24 h. The rehydrated liposomes were used for experiments after minimum three hours and up to three days after rehydration.

Electrophysiology

Glass pipettes [Drummond Scientific, Broomall, PA] were pulled with a Narishige gravity puller [PP-83; Narishige, Tokyo, Japan]. Patch solution (200 mM KCl, 40 mM $MgCl_2$, 5 mM Hepes-KOH, pH7.2) and bath solution (patch solution supplemented with 300 mM sucrose) were used in the recording. Currents were amplified with an Axopatch 200B amplifier (Axon Instruments), and data were acquired at a sampling rate of 5 kHz with 2 kHz filtration. Negative pressure ramp was applied with a high-pressure clamp apparatus (HSPC-1 ALA Scientific Instruments, USA) [39]. The recorded channel currents were analysed using the pClamp 10 analysis software (Molecular Devices, Sunnyvale, CA). Channel activation by pressure was fitted to the Boltzmann distribution function of the form $I = I_{max}/[1 + \exp \alpha (P_{mid} - P)]$, where I is the current, I_{max} is the maximum current, P is the negative pressure applied to the patch membrane, P_{mid} is the activation midpoint, and α is the channel sensitivity to pressure.

Measurement of glutamate release

The MscCG (NCgl1221) gene of *Corynebacterium glutamicum* ATCC 13869 was amplified using PCR and introduced in wild-type *Escherichia coli* strain using plasmid vector, pSTV29, that carried the lac promoter. The wild-type *E. coli* strain K-12 W3110 was used as the host and incubated on LB agar medium containing 50 mg/L chloramphenicol for 24 h at 37°C. The cells from one-sixth of the plate were harvested and inoculated in 20 mL MS medium containing 40 g/L glucose, 16 g/L $(NH_4)_2SO_4$, 1 g/L $MgSO_4 \cdot 7H_2O$, 1 g/L KH_2PO_4, 10 mg/L $MnSO_4 \cdot 4H_2O$, 10 mg/L $FeSO_4 \cdot 7H_2O$, 8 g/L yeast extract, 50 g/L $CaCl_2$, and 50 mg/L chloramphenicol. After 24 h of incubation at 37°C on a reciprocal shaker, the seed cultures were inoculated in 20 mL fresh MS medium with 0.1 mM isopropyl β-D-1-thiogalactopyranoside, with an optical density at 660 nm (OD_{660}) of 2.5. Cultures were incubated at 37°C on a reciprocal shaker and cell growth was monitored in terms of changes in OD_{660}. The amount of glutamate was enzymatically estimated using glutamate oxidase, which produces hydrogen peroxide, 2-oxoglutaric acid, and ammonia from glutamate [40]. The resulting hydrogen peroxide was used by peroxidase to produce a blue pigment from N-ethyl-N-(2-hydroxy-3-sulfopropyl)-3,5-dimethoxyaniline and 4-aminoantipyrine, which was estimated in terms of absorbance at OD_{660}

Acknowledgements

We thank Paul Rhode for his help with the purification of MscS-(C-MscCG). We also thank Dr Michelle Edwards and Prof Ian Booth for the generous donation of the *E. coli* strains MJF431 and MJF612. This work was supported by a Fellowship from the Japanese Society for Promotion of Science (JSPS) to YN and the Principal Research Fellowship (1044628) and a grant (107980) from the National Health and Medical Research Council of Australia to BM. This work was also supported in part by funds from the Office of Health and Medical Research, NSW State Government, Australia.

Author contributions:

Y. N., R. K., and B. M. designed experiments and wrote the manuscript. M.B. created the constructs of MscCG mutants and chimeric channel MscS-(C-MscCG). Y. N. and H. E. prepared *E. coli* spheroplasts for electrophysiology. T. K. measured the glutamate release from *E. coli*. Y. N. conducted the experiments and analysed data. B. M., R. K. and H. K. contributed new reagents/analytic tools. All authors reviewed and edited the manuscript.

Conflict of interest statement: The authors declare no conflict of interest.

Figure legends

Figure 1

The structural feature of MscCG and MscS A) Second structure of MscCG (top) and MscS (bottom) B) Sequence alignment between MscCG and MscS. Negatively charged residues are highlighted in black, and positively charged residues in TM1 of MscCG in grey.

Figure2

The effect of the C-terminal domain of MscCG in the activation threshold and conductance of MscCG and MscS in E. coli spheroplasts A) Current response of MscCG, MscCGΔ247, MscS, and MscS-(C-MscCG) when 8 s pressure ramp applied to the membrane at +40 mV. B) Activation threshold ratio between MscCG/MscS against MscL in the various range of voltage C) Current-voltage curve. All experiments were performed more than three times independently. Bars show S.E.

Figure 3

Current trace of MscCG having TM4 replaced with artificial transmembrane helix Current response under pressure ramp at +40 mV (top). Activation threshold ratio for opening (black) and closing (white) between MscCG and MscCG-hgTM4 (bottom). All experiments were performed independently more than three times. Bars show S.E. *; Student t-test, $P < 0.05$.

Figure 4

Slow closing by the C-terminal domain of MscCG on the gating of MscS A). Currents of MscS and MscS-(C-MscCG) under pulse-shaped pressure at +40 mV. B) Activation curve of

MscS and MscS-(C-MscCG) fitted by Boltzmann function. C) Current response of MscS and MscS-(C-MscCG) under 1, 3, 5, 7, 9 s pressure ramps at +40 mV. D) P_{mid} for opening and closing of MscS (left) and MscS-(C-MscCG) (right) in the range of pressure ramp rates are shown as closed circle and open circle, respectively. E) 1/α for opening and closing of MscS (left) and MscS-(C-MscCG) (right) under various pressure ramp rate are shown as closed circle and open circle.

Figure 5

Glutamate release via MscCG in *E. coli*. The cell growth (left) and the glutamate productivity (right) were measured in the *E. coli* strain. MscCG (closed circle) and empty vector (open circle) were introduced in the *E. coli* strain. All experiments were performed independently more than three times. Bars show S.E.

Figure 6

Gating hysteresis of MscS and MscS-(C-MscCG) in azolectin liposomes. A). The result of proteins purification on SDS-PAGE gel. Lane M: Marker, lane 1: MscS-(C-MscCG), lane 2: MscS. B). Voltage-dependent gating hysteresis of MscS-(C-MscCG). Voltage and pressure ramp were applied in the same patch membrane. C). The ratio between closing and opening threshold of MscS-(C-MscCG) (open circle) and MscS (closed circle) in the range of -80 mV to +120mV. D). The continuous opening of MscS-(C-MscCG) at high voltage. Voltage and pressure ramp were applied in the same patch membrane. All experiments were performed independently more than three times. Bars show S.E. *; Student t-test, $P < 0.05$.

Figure 7

Gating characteristics of MscS at high voltage. A) Current response of MscS in the range of pipette potential from -80 to +160 mV. Pressure ramp was applied in the same patch membrane. MscS remained open for more than 2 min after releasing pressure ramp at +160 mV. B) The single channel current of MscS in + 40, +80, +120, and +160 mV and pressure were applied in the same patch membrane. Fully open (FO) and Closed (C) level of a single channel is shown in each trace.

References

[1] I.R. Booth, P. Blount, The MscS and MscL families of mechanosensitive channels act as microbial emergency release valves, J Bacteriol 194 (2012) 4802-4809.

[2] C.D. Pivetti, M.R. Yen, S. Miller, W. Busch, Y.H. Tseng, I.R. Booth, M.H. Saier, Jr., Two families of mechanosensitive channel proteins, Microbiol Mol Biol Rev 67 (2003) 66-85, table of contents.

[3] S.I. Sukharev, B. Martinac, V.Y. Arshavsky, C. Kung, Two types of mechanosensitive channels in the Escherichia coli cell envelope: solubilization and functional reconstitution, Biophys J 65 (1993) 177-183.

[4] N. Levina, S. Totemeyer, N.R. Stokes, P. Louis, M.A. Jones, I.R. Booth, Protection of Escherichia coli cells against extreme turgor by activation of MscS and MscL mechanosensitive channels: identification of genes required for MscS activity, EMBO J 18 (1999) 1730-1737.

[5] K. Kamaraju, V. Belyy, I. Rowe, A. Anishkin, S. Sukharev, The pathway and spatial scale for MscS inactivation, J Gen Physiol 138 (2011) 49-57.

[6] T. Nomura, M. Sokabe, K. Yoshimura, Interaction between the cytoplasmic and transmembrane domains of the mechanosensitive channel MscS, Biophys J 94 (2008) 1638-1645.

[7] M. Boer, A. Anishkin, S. Sukharev, Adaptive MscS gating in the osmotic permeability response in E. coli: the question of time, Biochemistry 50 (2011) 4087-4096.

[8] Y. Nakayama, K. Fujiu, M. Sokabe, K. Yoshimura, Molecular and electrophysiological characterization of a mechanosensitive channel expressed in the chloroplasts of Chlamydomonas, Proc Natl Acad Sci U S A 104 (2007) 5883-5888.

[9] Y. Nakayama, K. Yoshimura, H. Iida, Organellar mechanosensitive channels in fission yeast regulate the hypo-osmotic shock response, Nat Commun 3 (2012) 1020.

[10] E.S. Haswell, E.M. Meyerowitz, MscS-like proteins control plastid size and shape in Arabidopsis thaliana, Curr Biol 16 (2006) 1-11.

[11] K.M. Veley, S. Marshburn, C.E. Clure, E.S. Haswell, Mechanosensitive channels protect plastids from hypoosmotic stress during normal plant growth, Curr Biol 22 (2012) 408-413.

[12] M.E. Wilson, G. Maksaev, E.S. Haswell, MscS-like mechanosensitive channels in plants and microbes, Biochemistry 52 (2013) 5708-5722.

[13] E. Radmacher, K.C. Stansen, G.S. Besra, L.J. Alderwick, W.N. Maughan, G. Hollweg, H. Sahm, V.F. Wendisch, L. Eggeling, Ethambutol, a cell wall inhibitor of Mycobacterium tuberculosis, elicits L-glutamate efflux of Corynebacterium glutamicum, Microbiology 151 (2005) 1359-1368.

[14] K. Hashimoto, H. Kawasaki, K. Akazawa, J. Nakamura, Y. Asakura, T. Kudo, E. Sakuradani, S. Shimizu, T. Nakamatsu, Changes in composition and content of

mycolic acids in glutamate-overproducing Corynebacterium glutamicum, Biosci Biotechnol Biochem 70 (2006) 22-30.

[15] M.A. Laneelle, M. Tropis, M. Daffe, Current knowledge on mycolic acids in Corynebacterium glutamicum and their relevance for biotechnological processes, Appl Microbiol Biotechnol 97 (2013) 9923-9930.

[16] C. Hoischen, R. Kramer, Membrane alteration is necessary but not sufficient for effective glutamate secretion in Corynebacterium glutamicum, J Bacteriol 172 (1990) 3409-3416.

[17] J. Nakamura, S. Hirano, H. Ito, M. Wachi, Mutations of the Corynebacterium glutamicum NCgl1221 gene, encoding a mechanosensitive channel homolog, induce L-glutamic acid production, Appl Environ Microbiol 73 (2007) 4491-4498.

[18] K. Börngen, A.R. Battle, N. Moker, S. Morbach, K. Marin, B. Martinac, R. Krämer, The properties and contribution of the Corynebacterium glutamicum MscS variant to fine-tuning of osmotic adaptation, Biochim Biophys Acta 1798 (2010) 2141-2149.

[19] K. Hashimoto, J. Murata, T. Konishi, I. Yabe, T. Nakamatsu, H. Kawasaki, Glutamate is excreted across the cytoplasmic membrane through the NCgl1221 channel of Corynebacterium glutamicum by passive diffusion, Biosci Biotechnol Biochem 76 (2012) 1422-1424.

[20] M. Becker, K. Börngen, T. Nomura, A.R. Battle, K. Marin, B. Martinac, R. Krämer, Glutamate efflux mediated by Corynebacterium glutamicum MscCG, Escherichia coli MscS, and their derivatives, Biochim Biophys Acta 1828 (2013) 1230-1240.

[21] H.R. Malcolm, J.A. Maurer, The mechanosensitive channel of small conductance (MscS) superfamily: not just mechanosensitive channels anymore, Chembiochem 13 (2012) 2037-2043.

[22] K. Hashimoto, K. Nakamura, T. Kuroda, I. Yabe, T. Nakamatsu, H. Kawasaki, The protein encoded by NCgl1221 in Corynebacterium glutamicum functions as a mechanosensitive channel, Biosci Biotechnol Biochem 74 (2010) 2546-2549.

[23] Y. Nakayama, K. Yoshimura, H. Iida, Electrophysiological characterization of the mechanosensitive channel MscCG in Corynebacterium glutamicum, Biophys J 105 (2013) 1366-1375.

[24] C. Yamashita, K. Hashimoto, K. Kumagai, T. Maeda, A. Takada, I. Yabe, H. Kawasaki, M. Wachi, L-Glutamate secretion by the N-terminal domain of the Corynebacterium glutamicum NCgl1221 mechanosensitive channel, Biosci Biotechnol Biochem 77 (2013) 1008-1013.

[25] C.D. Cox, Y. Nakayama, T. Nomura, B. Martinac, The evolutionary 'tinkering' of MscS-like channels: generation of structural and functional diversity, Pflugers Arch 467 (2015) 3-13.

[26] M. Becker, R. Krämer, MscCG from Corynebacterium glutamicum: Functional significance of the C-terminal domain, European Biophysics Journal in press (2015).

[27] I. Nasie, S. Steiner-Mordoch, A. Gold, S. Schuldiner, Topologically Random Insertion of EmrE Supports a Pathway for Evolution of Inverted Repeats in Ion-coupled Transporters, Journal of Biological Chemistry 285 (2010) 15234-15244.

[28] N. Ozcan, C.S. Ejsing, A. Shevchenko, A. Lipski, S. Morbach, R. Krämer, Osmolality, temperature, and membrane lipid composition modulate the activity of betaine transporter BetP in Corynebacterium glutamicum, J Bacteriol 189 (2007) 7485-7496.

[29] T. Nomura, C.G. Cranfield, E. Deplazes, D.M. Owen, A. Macmillan, A.R. Battle, M. Constantine, M. Sokabe, B. Martinac, Differential effects of lipids and lyso-lipids on the mechanosensitivity of the mechanosensitive channels MscL and MscS, Proc Natl Acad Sci U S A 109 (2012) 8770-8775.

[30] P. Ridone, Y. Nakayama, B. Martinac, A.R. Battle, Patch clamp characterization of the effect of cardiolipin on MscS of E. coli, Eur Biophys J (2015).

[31] R.K. Christian Hoischen, Evidence for an efflux carrier system involved in the secretion of glutamate by Corynebacterium glutamicum, Archives of Microbiology 151 (1989) 342-347.

[32] B. Martinac, M. Buechner, A.H. Delcour, J. Adler, C. Kung, Pressure-sensitive ion channel in Escherichia coli, Proc Natl Acad Sci U S A 84 (1987) 2297-2301.

[33] G. Maksaev, E. S. Haswell, MscS-Like10 is a stretch-activated ion channel from Arabidopsis thaliana with a preference for anions. *Proc Natl Acad Sci U S A.* 2012 109:19015-19020. doi: 10.1073/pnas.1213931109.

[34]C.D. Cox, T. Nomura, C.S. Ziegler, A.K. Campbell, K.T. Wann, B. Martinac, Selectivity mechanism of the mechanosensitive channel MscS revealed by probing channel subconducting states, Nat Commun 4 (2013) 2137.

[35]U. Schumann, M.D. Edwards, T. Rasmussen, W. Bartlett, P. van West, I.R. Booth, YbdG in Escherichia coli is a threshold-setting mechanosensitive channel with MscM activity, Proc Natl Acad Sci U S A 107 (2010) 12664-12669.

[36] B. Martinac, P.R. Rohde, C.G. Cranfield, T. Nomura, Patch clamp electrophysiology for the study of bacterial ion channels in giant spheroplasts of E. coli, Methods Mol Biol 966 (2013) 367-380.

[37] C.C. Häse, A.C. Le Dain, B. Martinac, Purification and functional reconstitution of the recombinant large mechanosensitive ion channel (MscL) of Escherichia coli, J Biol Chem 270 (1995) 18329-18334.

[38] A.H. Delcour, B. Martinac, J. Adler, C. Kung, Modified reconstitution method used in patch-clamp studies of Escherichia coli ion channels, Biophys J 56 (1989) 631-636.

[39] S.R. Besch, T. Suchyna, F. Sachs, High-speed pressure clamp, Pflugers Arch 445 (2002) 161-166.

[40] H. Kusakabe, Y. Midorikawa, T. Fujishima, A. Kuninaka and H. Yoshino, Purification and properties of a new enzyme, L-Glutamate oxidase, from Streptomyces sp. X-l1.9-6 grown on wheat branf, Agric. Biol Chem., 47 (1983) 1323-1328.

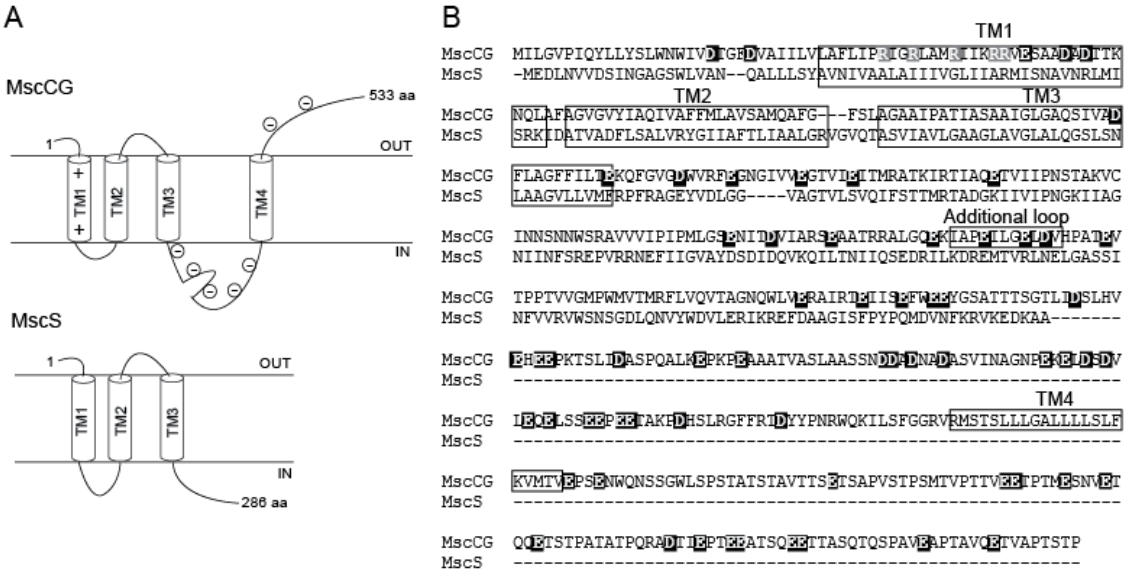
A
MscCG
533 aa
1
OUT
TM1
TM2
TM3
TM4
IN
MscS
1
OUT
TM1
TM2
TM3
IN
286 aa
B
TM1
MscCG MILGVPIQYLLYSLWNWIVDIGRDVAIILVLAFLIPRIGRLAMRIIKRRMESAADPDITK
MscS -MEDLNVVDSINGAGSWLVAN--QALLLSYAVNIVAALAIIIVGLIIARMISNAVNRLMI
TM2 TM3
MscCG NQLAFAGVGVYIAQIVAFFMLAVSAMQAFG---FSLAGAAIPATIASAAIGLGAQSIVAD
MscS SRKIDATVADFLSALVRYGIIAFTLIAALGRVGVQTASVIAVLGAAGLAVGLALQGSLSN
MscCG FLAGFFILDEKQFGVQDWVRFEGNGIVVEGTVIEITMRATKIRTIAQETVIIPNSTAKVC
MscS LAAGVLLVMERPFRAGEYVDLGG----VAGTVLSVQIFSTTMRTADGKIIVIPNGKIIAG
Additional loop
MscCG INNSNNWSRAVVVIPIPMLGSEQNITDVIARSEAATRRALGQEKTAPEILGEEDVHPATEV
MscS NIINFSREPVRRNEFIIGVAYDSDIDQVKQILTNIIQSEDRILKDREMTVRLNELGASSI
MscCG TPPTVVGMPWMVTMRFLVQVTAGNQWLVERAIRTEIISEFWEEGYGSATTSGTLIDSLHV
MscS NFVVRVWSNSGDLQNVYWDVLERIKREFDAAGISFPYPQMDVNFKRVKEDKAA-------
MscCG EHEEPKTSLIDASPQALKEPKPEAAATVASLAASSNDDADNADASVINAGNPEKEELDSDV
MscS ----------
TM4
MscCG IEQELSSEEPEETAKEDHSLRGFFRTDYYPNRWQKILSFGGRVRMSTSLLLGALLLLSLF
MscS ----------
MscCG KVMTVEPSENWQNSSGWLSPSTATSTAVTTSETSAPVSTPSMTVPTTVEETPTMESNVET
MscS ----------
MscCG QQETSTPATATPQRADTTDEPTEEATSQEETTASQTQSPAVEAPTAVQETVAPTSTP
MscS ----------

Figure 1

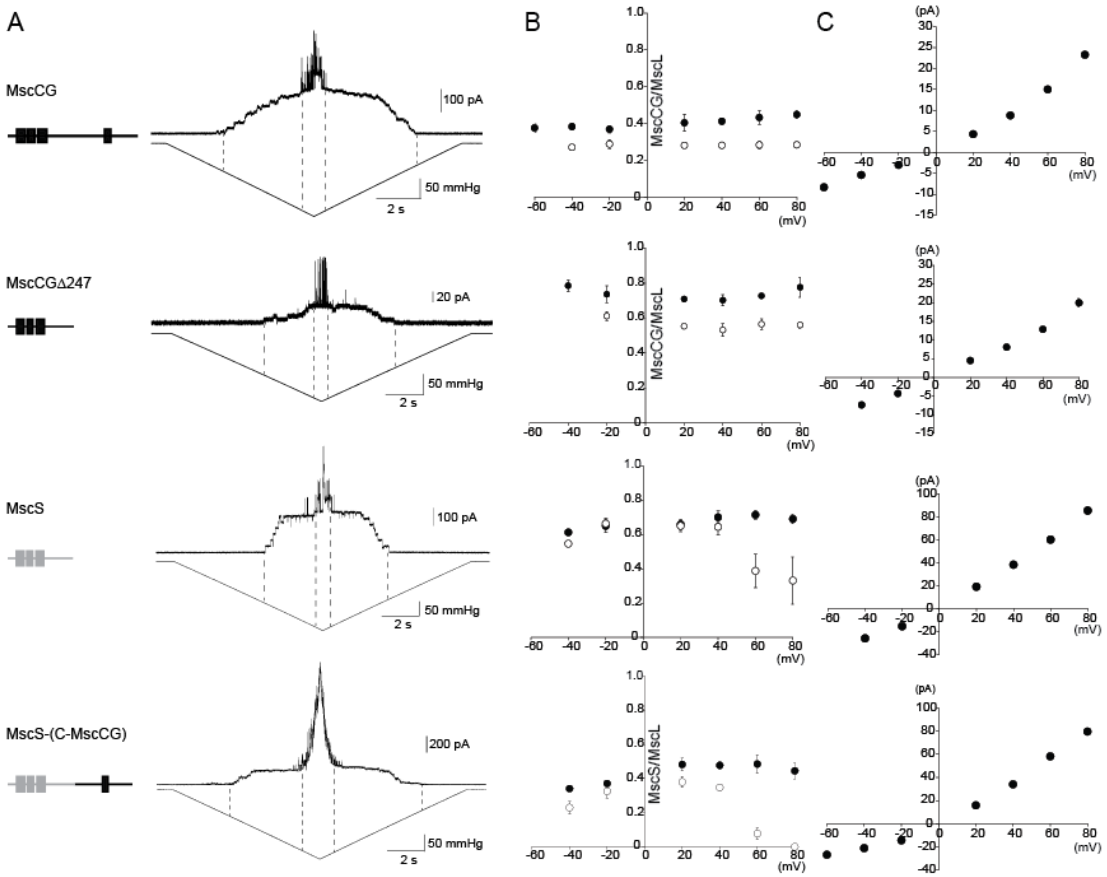
A
MscCG
100 pA
50 mmHg
2 s
MscCGΔ247
20 pA
50 mmHg
2 s
MscS
100 pA
50 mmHg
2 s
MscS-(C-MscCG)
200 pA
50 mmHg
2 s
B
MscCG/MscL
MscCG/MscL
MscCG/MscL
MscS/MscL
(mV)
C
(pA)
(mV)

Figure 2

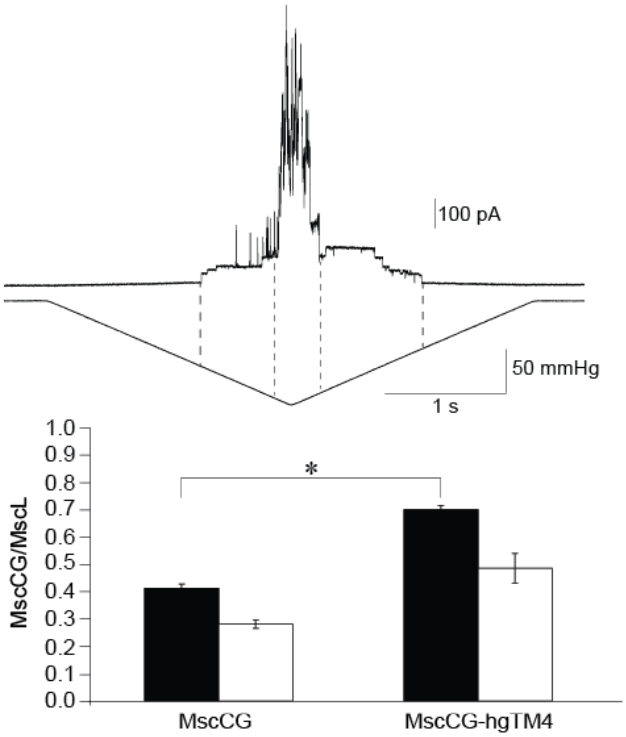
100 pA
50 mmHg
1 s
MscCG/MscL
1.0
0.9
0.8
0.7
0.6
0.5
0.4
0.3
0.2
0.1
0.0
*
MscCG
MscCG-hgTM4

Figure 3

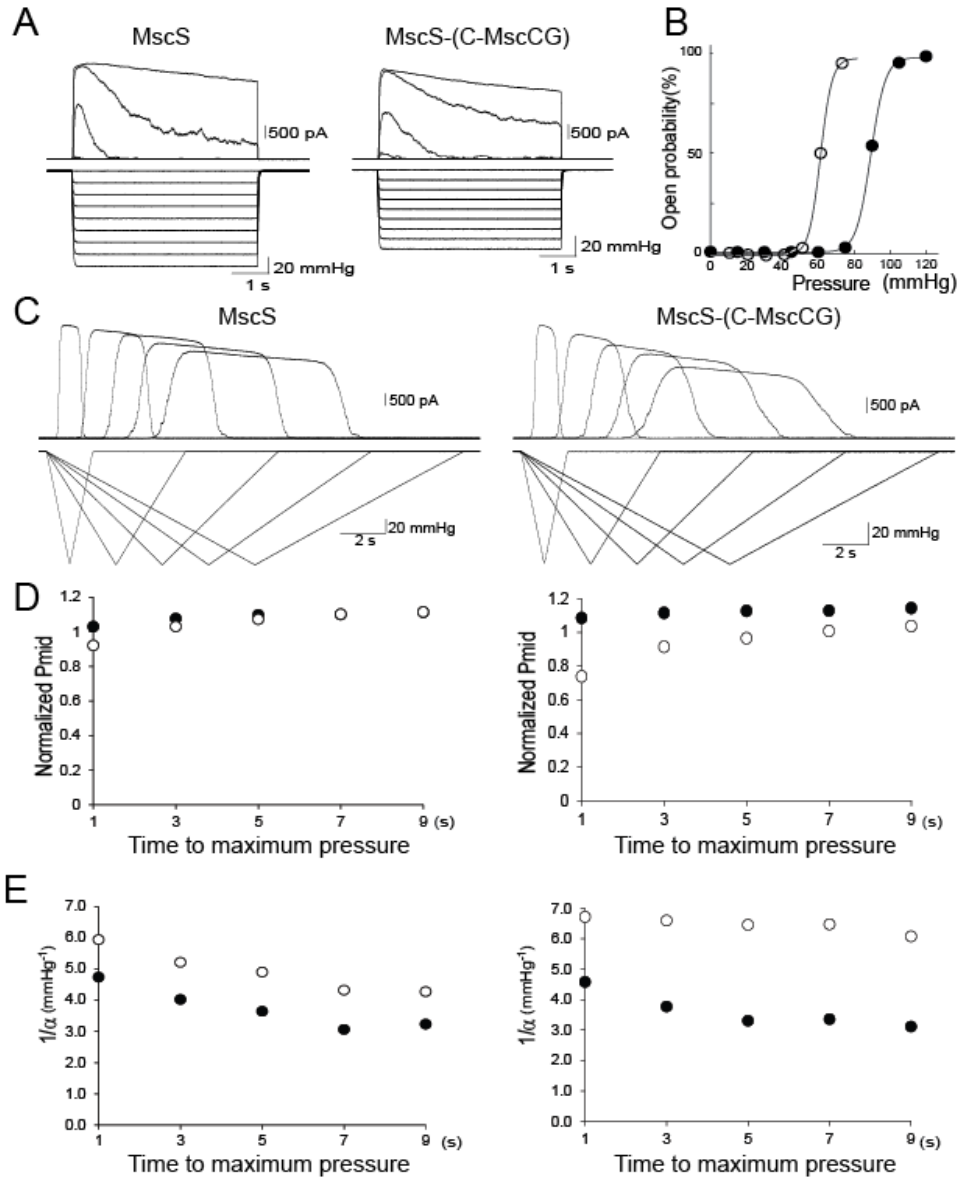
A
MscS
MscS-(C-MscCG)
500 pA
20 mmHg
1 s
B
Open probability(%)
Pressure (mmHg)
C
MscS
MscS-(C-MscCG)
2 s
D
Normalized Pmid
Time to maximum pressure
(s)
E
1/α (mmHg⁻¹)
Time to maximum pressure

Figure 4

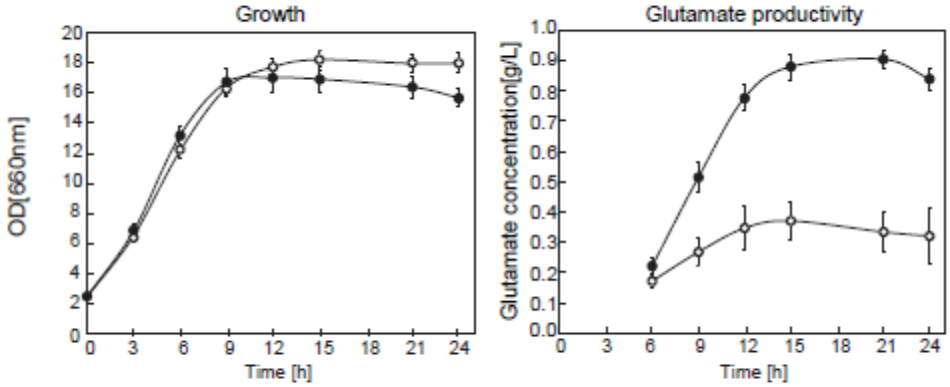
Growth
OD[660nm]
Time [h]
Glutamate productivity
Glutamate concentration[g/L]
Time [h]

Figure 5

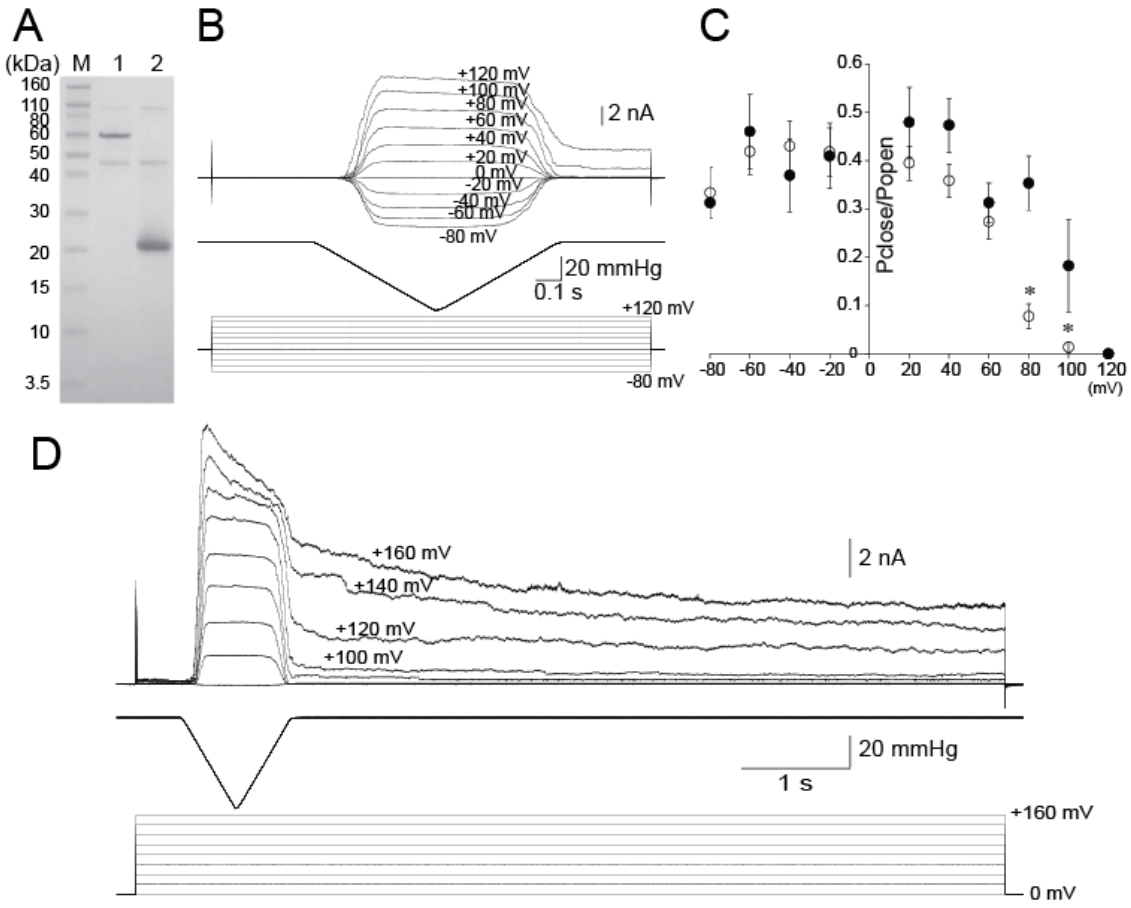
A
(kDa) M 1 2
160
110
80
60
50
40
30
20
15
10
3.5
B
+120 mV
+100 mV
+80 mV
+60 mV
+40 mV
+20 mV
0 mV
-20 mV
-40 mV
-60 mV
-80 mV
2 nA
20 mmHg
0.1 s
+120 mV
-80 mV
C
Pclose/Popen
0.6
0.5
0.4
0.3
0.2
0.1
0
-80 -60 -40 -20 0 20 40 60 80 100 120
(mV)
*
*
D
+160 mV
+140 mV
+120 mV
+100 mV
2 nA
20 mmHg
1 s
+160 mV
0 mV

Figure 6

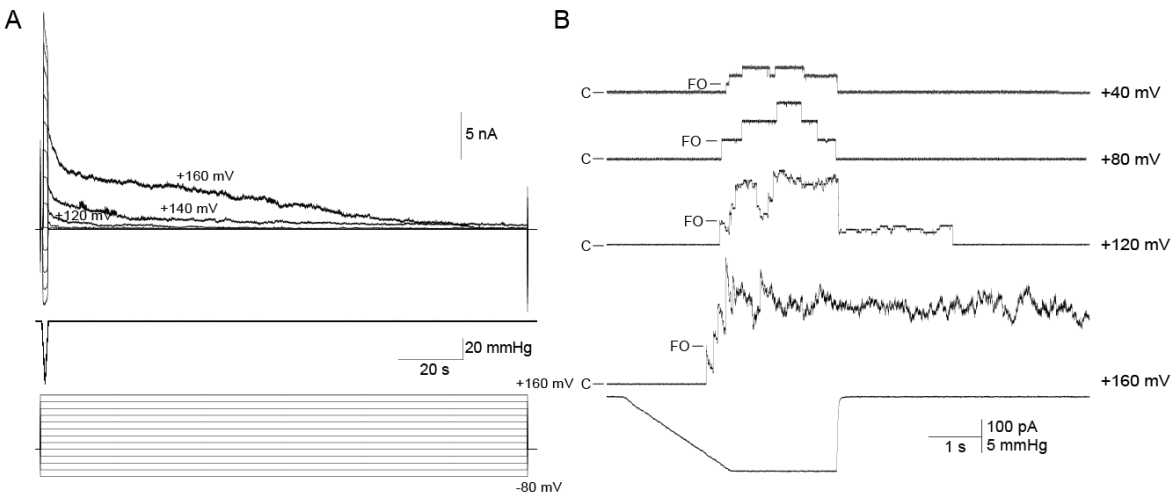
A
5 nA
+160 mV
+140 mV
+120 mV
20 mmHg
20 s
+160 mV
-80 mV
B
C
FO
+40 mV
+80 mV
+120 mV
+160 mV
100 pA
5 mmHg
1 s

Figure 7